

1   **Title: An antibody-dependent enhancement (ADE) activity eliminated neutralizing  
2   antibody with potent prophylactic and therapeutic efficacy against SARS-CoV-2 in rhesus  
3   monkeys**

4

5   **Authors:**

6   Shuang Wang<sup>1,7, 8</sup>, Yun Peng<sup>2, 8</sup>, Rongjuan Wang<sup>1,7, 8</sup>, Shasha Jiao<sup>1,7, 8</sup>, Min Wang<sup>1, 8</sup>, Weijin  
7   Huang<sup>3, 8</sup>, Chao Shan<sup>4</sup>, Wen Jiang<sup>1</sup>, Zepeng Li<sup>1</sup>, Chunying Gu<sup>1</sup>, Ben Chen<sup>1</sup>, Xue Hu<sup>4</sup>, Yanfeng  
8   Yao<sup>2</sup>, Juan Min<sup>5</sup>, Huajun Zhang<sup>2</sup>, Ying Chen<sup>2</sup>, Ge Gao<sup>2</sup>, Peipei Tang<sup>1</sup>, Gang Li<sup>1</sup>, An Wang<sup>1</sup>, Lan  
9   Wang<sup>3</sup>✉, Shuo Chen<sup>6</sup>✉, Xun Gui<sup>1</sup>✉, Jinchao Zhang<sup>1</sup>✉, Zhiming Yuan<sup>2</sup>✉, Datao Liu<sup>1</sup>✉

10

11   **Affiliations:**

12   <sup>1</sup>Mabwell (Shanghai) Bioscience Co., Ltd., Shanghai, 201210, China.

13   <sup>2</sup>Center for Biosafety Mega-Science, Wuhan Institute of Virology, Chinese Academy of  
14   Sciences, Wuhan, Hubei, 430071, China.

15   <sup>3</sup>Key Laboratory of the Ministry of Health for Research on Quality and Standardization of  
16   Biotech Products, National Institutes for Food and Drug Control, Beijing, 100050, China.

17   <sup>4</sup>State Key Laboratory of Virology, Wuhan Institute of Virology, Chinese Academy of Sciences,  
18   Wuhan, Hubei, 430071, China.

19   <sup>5</sup>Wuhan Institute of Virology, Chinese Academy of Sciences, Wuhan, Hubei, 430071, China.

20   <sup>6</sup>Ludwig Cancer Research, Nuffield Department of Medicine, University of Oxford, Oxford  
21   OX3 7DQ, United Kingdom.

22   <sup>7</sup>Beijing Kohnoor Science & Technology Co., Ltd., Beijing, 102206, China.

23   <sup>8</sup>These authors contributed equally: Shuang Wang, Yun Peng, Rongjuan Wang, Shasha Jiao,  
24   Min Wang, Weijin Huang.

25   ✉Email: [wanglan@nifdc.org.cn](mailto:wanglan@nifdc.org.cn); [ericshuochen@gmail.com](mailto:ericshuochen@gmail.com); [xun.gui@mabwell.com](mailto:xun.gui@mabwell.com);

26   [jinchao.zhang@mabwell.com](mailto:jinchao.zhang@mabwell.com); [yzm@wh.iov.cn](mailto:yzm@wh.iov.cn); [datao.liu@mabwell.com](mailto:datao.liu@mabwell.com)

27

28

29 **Abstract:**

30 Efficacious interventions are urgently needed for the treatment of COVID-19. Here, we report  
31 a monoclonal antibody (mAb), MW05, showing high SARS-CoV-2 neutralizing activity by  
32 disrupting the interaction of receptor binding domain (RBD) with angiotensin-converting  
33 enzyme 2 (ACE2) receptor. Crosslinking of Fc with Fc $\gamma$ RIIB mediates antibody-dependent  
34 enhancement (ADE) activity by MW05. This activity was eliminated by introducing the LALA  
35 mutation to the Fc region (MW05/LALA). Most importantly, potent prophylactic and  
36 therapeutic effects against SARS-CoV-2 were observed in rhesus monkeys. A single dose of  
37 MW05/LALA completely blocked the infection of SARS-CoV-2 in a study of its prophylactic  
38 effect and totally cleared SARS-CoV-2 in three days in a treatment setting. These results pave  
39 the way for the development of MW05/LALA as an effective strategy for combating COVID-  
40 19.

41

42 COVID-19, caused by SARS-CoV-2, is currently spreading globally, threatening human  
43 health and economic development <sup>1,2</sup>. As of July 27, 2020, COVID-19 has resulted in more than  
44 16 million infections and 647,784 deaths. Although, multiple clinical trials are ongoing to  
45 evaluate repurposing anti-viral and anti-inflammatory agents, no specific treatment against  
46 SARS-CoV-2 has been approved since the worldwide outbreak began six months ago <sup>3</sup>.  
47 Treatments using plasma from convalescent COVID-19 patients have shown clear clinical  
48 improvement of both mild and severe cases of COVID-19, indicating that passive  
49 administration of neutralizing mAbs could have a major impact on controlling the SARS-CoV-  
50 2 pandemic by providing immediate protection <sup>4,5</sup>. During the SARS and Middle East  
51 respiratory syndrome coronavirus (MERS-CoV) outbreaks, a number of neutralizing mAbs  
52 were developed and proved their potential therapeutic uses for the treatment of coronavirus  
53 infections <sup>6,7</sup>. Neutralizing antibodies for Ebola virus, mAb114 and REGN-EB3, are other  
54 encouraging examples that using antibody-based therapy can be effective during an infectious  
55 disease outbreak <sup>8-10</sup>.

56 The spike (S) protein on the surface of SARS-CoV-2 is the major molecular determinant  
57 for viral attachment, membrane fusion and entry into host cells. Therefore, this protein is the  
58 main target for development of neutralizing antibodies and vaccines. Previous studies revealed  
59 that a large number of antibodies targeting the receptor binding domain (RBD) of either SARS-  
60 CoV or MERS-CoV showed potent neutralizing activities by disrupting the interaction of spike  
61 protein with receptors on host cells <sup>11-13</sup>. Screening of RBD targeting antibodies is the most  
62 straightforward way to generate SARS-CoV-2 neutralizing antibodies.

63 To obtain fully human SARS-CoV-2 neutralizing mAbs, we first generated SARS-CoV-2

64 RBD recombinant protein. We used this protein as bait to isolate specific memory B cells from  
65 peripheral blood mononuclear cells (PBMCs) of a COVID-19 convalescent patient. We then  
66 used a single B cell cloning strategy to amplify the variable regions of IgG antibodies from  
67 individual B cells and insert them into human IgG1 vectors for recombinant antibody  
68 expression <sup>14</sup>. A large panel of SARS-CoV-2 RBD-binding mAbs were generated and  
69 characterized. Two mAbs, MW05 and MW07, showed high RBD binding abilities and strong  
70 RBD/ACE2 disrupting activities in ELISA. IC<sub>50</sub> was determined to be 0.054 µg/mL for MW05  
71 and 0.037 µg/mL for MW07. (Fig. 1 A to C). FACS analysis showed that both mAbs could  
72 specifically bind to SARS-CoV-2 S protein expressed on HEK293 cells (Fig. 1D). The  
73 dissociation constants (K<sub>d</sub>) of MW05 and MW07 binding to SARS-CoV-2 S1 recombinant  
74 protein was measured by a surface plasmon resonance (SPR) assay. K<sub>d</sub> was 0.403 nM for  
75 MW05 and 0.462 nM for MW07 (Fig.1E). No cross reactivity with SARS-CoV or MERS-CoV  
76 S1 recombinant proteins was detected for either mAb, as assessed using ELISA (Fig. 1 F).  
77 SARS-CoV-2 raced around the world after its initial outbreak. Over the past few months it has  
78 been mutating. We next expressed RBD recombinant proteins from eight SARS-CoV-2 strains  
79 with reported high-frequency mutations. Binding assays showed that both MW05 and MW07  
80 exhibited the same binding abilities to all RBD recombinant proteins. This result suggests that  
81 MW05 and MW07 may neutralize all eight of these strains (Fig. 1G; Extended Data Fig. 1).

82 To investigate the neutralizing activities of MW05 and MW07, we used *in vitro* assays to  
83 assess neutralization of first pseudovirus bearing the S protein of SARS-CoV-2 and then  
84 authentic virus. Both MW05 and MW07 inhibited pseudovirus infection of Huh7 cells  
85 effectively. NT<sub>50</sub> was measured as 0.030 µg/ml for MW05 and 0.063 µg/ml for MW07 (Fig. 2,

86 A and B). We further evaluated the neutralizing activities of these two mAbs with authentic  
87 SARS-CoV-2 infection of Vero E6 cells. As expected, MW05 and MW07 blocked authentic  
88 SARS-CoV-2 entry into Vero E6 cells, with 100% neutralization titer (NT<sub>100</sub>) around 1 µg/ml  
89 for MW05 and 5 µg/ml for MW07 (Fig. 2, C and D). In summary, MW05 and MW07 exhibited  
90 substantial neutralization of both SARS-CoV-2 pseudovirus and authentic virus.

91 ADE has been observed for coronaviruses and several publications have shown that sera  
92 induced by SARS-CoV S protein enhanced viral entry into immune cells and inflammation<sup>15,16</sup>.

93 To evaluate ADE activities of MW05 and MW07, we assessed the infection of SARS-CoV-2  
94 pseudovirus and mAbs complex in THP-1, K562 and Raji cells. These cells are resistant to  
95 SARS-CoV-2 pseudovirus infection, as they do not express ACE2 receptor (Extended Data Fig.

96 2). Cells were incubated with the mixture of pseudovirus with serially diluted MW05. Enhanced  
97 SARS-CoV-2 pseudovirus infection of Raji cells, but not of THP-1 or K562 cells was observed  
98 (Fig. 3A). Interestingly, No ADE activity was detected for MW07 on all three cell lines (Fig.

99 3B). Next, we determined the FcγR expression profile of the three cell lines. FACS data  
100 revealed that Raji cells, which showed ADE activity for MW05, only express a relatively high  
101 level of FcγRIIB; THP-1 cells express high levels of FcγRIA and FcγRIIA; and K562 cells only  
102 express high level of FcγRIIA (Fig. 3C). These results indicate that FcγRIIB is the major FcγR  
103 contributing to the enhancement of SARS-CoV-2 infection mediated by MW05.

104 To further assess the ADE activities of MW05, we pre-incubated Raji cells along with  
105 irrelevant hIgG1 or MW05 along with FcγRIA recombinant protein to disrupt the interaction of  
106 MW05 Fc with FcγRIIB on Raji cells. Both pre-incubation strategies effectively inhibited the  
107 ADE activities of MW05 (Fig. 3D and E). FcγRIA has high affinity for the Fc of human IgG1.

108 Accordingly, pre-incubation of MW05 with Fc $\gamma$ RIA recombinant protein showed higher ADE  
109 inhibition than did pre-incubation of irrelevant hIgG1 with Raji cells by disruption of MW05 Fc  
110 with Fc $\gamma$ RIIB on Raji cells (Fig. 3 D and E). To eliminate the risk of ADE and Fc-  
111 mediated acute lung injury *in vivo*, we introduced the LALA mutation to the Fc region of MW05  
112 (MW05/LALA) to decrease the engagement of MW05 with Fc $\gamma$ Rs. This mutation completely  
113 eliminated ADE activity of MW05 without decreasing its neutralizing activity (Fig. 3 F and G).

114 We evaluated the prophylactic and therapeutic effects of MW05/LALA in a rhesus monkey  
115 SARS-CoV-2 infection model. In the prophylactic (pre-challenge) group, three animals were  
116 injected intravenously with a single dose of MW05/LALA (20 mg/kg) one day before receiving  
117 a  $1 \times 10^5$  50% tissue culture infectious dose (TCID<sub>50</sub>) SARS-CoV-2 challenge via intratracheal  
118 incubation (Fig. 4A). MW05/LALA antibody effectively protected animals from SARS-CoV-2  
119 infection; almost no virus was detected in the oropharyngeal swabs of the prophylactic group  
120 (Fig. 4B).

121 In the treatment (post-challenge) group, three animals were first challenged with  $1 \times 10^5$   
122 TCID<sub>50</sub> SARS-CoV-2. Then, at day 1 post infection (dpi), a single dose of MW05/LALA (40  
123 mg/kg) was administered intravenously to these animals (Fig. 4A). Animals in the control group  
124 (n=3) were given a single dose of irrelevant hIgG1 (20 mg/kg) on 1 dpi. In the control group,  
125 the viral loads in oropharyngeal swabs increased to a peak of about  $10^{7.0}$  RNA copies/mL on 4  
126 dpi, then decreased to the limit of detection on 7 dpi (Fig. 4B). Virus was only detected in the  
127 rectal swabs of two animals in the control group (Fig. 4C). Notably, virus titers decreased in  
128 the MW05/LALA treatment group immediately after administration. No virus was detected in  
129 the MW05/LALA treatment group even on 4 dpi, the time point at which viral titers in the

130 control group reached their peak. A single dose of MW05/LALA exhibited SARS-CoV-2  
131 therapeutic efficacy in a rhesus monkey model, clearing virus in three days after antibody  
132 administration (Fig. 4B). No significant weight loss or body temperature change was observed  
133 in any of the animals during the study (Extended Data Fig. 3 and 4). No virus was detected in  
134 nasal swabs or blood samples (Extended Data Fig. 5). Additionally, no significant abnormal  
135 hematology changes were observed (Extended Data Fig. 6).

136 Rhesus monkeys challenged with SARS-CoV-2 were evaluated for tissue damage. One  
137 monkey from each group was euthanized for necropsy on 6 and 7 dpi. Interstitial pneumonia  
138 symptoms were observed in the control group, including thickened alveolar septa, intensive  
139 infiltration of monocytes and lymphocytes, and proliferation of fibroblasts (Fig. 4D). We also  
140 observed cellulose exudation in some alveolar cavities, with the formation of hyaline membrane  
141 and pulmonary hemorrhaging (Fig. 4D). Monkeys in treatment group displayed limited  
142 pathological lung changes, with overall alveolar structure intact and much lower levels of  
143 fibroblasts proliferation and leukocyte infiltration than were observed in the control monkeys  
144 (Fig. 4D). No lesions were observed in the lungs of the animal euthanized on 6 dpi and very  
145 mild pulmonary hemorrhaging of the animal euthanized on 7 dpi in the prophylactic group (Fig.  
146 4D). In summary, MW05/LALA effectively inhibited lung tissue damage in both prophylactic  
147 and therapeutic ways in a rhesus monkey SARS-CoV-2 infection model.

148 Immunohistochemical analysis of virus in lung tissues showed that SARS-CoV-2 protein  
149 only been detected in the lung tissue of the control group on 5 dpi but not 6 dpi and 7 dpi. In  
150 comparison, viral proteins were undetectable in the lung tissues of animals in the prophylactic  
151 and therapeutic groups (Fig. 4E). In order to further understand the distribution of SARS-CoV-

152 2 in upper respiratory tract, trachea and bronchus tissue samples were collected on 6 dpi and 7  
153 dpi. Viral titers were then determined by qRT-PCR. On 6 dpi and 7 dpi, high levels of SARS-  
154 CoV-2 RNA copies were detected in trachea and bronchi tissues of control animals, while no  
155 viral nucleic acid was detected from tissue samples of both prophylactic and therapeutic groups  
156 (Fig. 4F).

157 The global COVID-19 pandemic is running rampant over the world. There are great unmet  
158 medical needs for COVID-19 therapy as no SARS-CoV-2 specific drugs or vaccines have yet  
159 been approved. Neutralizing mAbs are promising agents to combat emerging infectious  
160 diseases. Our results showed the prophylactic and therapeutic efficacy of MW05/LALA on  
161 SARS-CoV-2 *in vivo*. This work paves the way for further development of antibody-based  
162 therapies for prophylactic or therapeutic treatment of COVID-19.

163

## 164 **Methods**

165 **Ethics statement.** All neutralizing assays using SARS-CoV-2 authentic virus were performed in  
166 biosafety level 3 (BSL-3) facility. Monkey studies were carried out in an animal biosafety level 4  
167 (ABSL-4) facility with protocols approved by the Laboratory Animal Welfare and Ethics Committee  
168 of the Chinese Academy of Sciences. The blood was taken from a convalescent COVID-19 patient  
169 after got his signature for the informed consent form.

170

171 **Cells and viruses.** HEK293 (ATCC, CRL-3216) cells, Huh7 (Institute of Basic Medical Sciences  
172 CAMS, 3111C0001CCC000679) cells and Vero E6 (ATCC, CRL-1586) cells were cultured at 37 °C  
173 in Dulbecco's Modified Eagle medium (DMEM) supplemented with 10% fetal bovine serum (FBS).

174 Raji (ATCC, CCL-86) cells, THP-1 (ATCC, TIB-202) cells and K562 (ATCC, CCL-243) cells were  
175 cultured at 37 °C in RPMI 1640 Medium with 10% FBS. SARS-CoV-2 was isolated by the Center  
176 for Disease Control and Prevention of Zhejiang province. Vero E6 cells were applied to the  
177 reproduction of SARS-CoV-2 stocks.

178

179 **Recombinant protein generation.** The SARS-CoV-2 RBD (319-533aa, accession number:  
180 QHD43416.1) , SARS-CoV-2 S1 (1-685aa, accession number: QHD43416.1) and SARS-CoV-2  
181 RBD mutants recombinant proteins tagged with C-terminal 6 × His were cloned into the pKN293E  
182 expression vector. HEK293 cells were transiently transfected with plasmids using 293fectinTM  
183 Transfection Reagent (Cat: 12347019, Life Technologies) when the cell density reached  $1 \times 10^6$   
184 cells/mL. Four days after transfection, the conditioned media was collected by centrifugation  
185 followed by purification using HisTrapTM HP (Cat: 17-5248-01, GE Healthcare). The purified  
186 protein was buffer exchanged into PBS using a Vivacon 500 concentrator (Cat: VS0122, Sartorius  
187 Stedim). For the generation of human ACE2-hFc and SARS-CoV-2 RBD-mFc recombinant  
188 proteins , RBD or ACE2 sequence (1-615aa, accession number: NP\_068576.1) was cloned into  
189 mouse IgG1 or human IgG1 Fc backbone in pKN293E expression vectors and transiently  
190 transfected into HEK293 cells followed by media collection and purification using MabSelect SuRe  
191 antibody purification resin (Cat: 29-0491-04, GE Healthcare). SEC-HPLC and SDS-PAGE were  
192 used to check the size and purity of these recombinant proteins.

193 SARS-CoV-2 RBD mutant information:

Mutants	Virus Strain Name	Accession ID	Data Source
---------	-------------------	--------------	-------------

RBD/NE39K	hCoV-19/Scotland/EDB162/2020	EPI_ISL_425924	GISAID
V367F	HCoV-19/England/20134027504/2020	EPI_ISL_423136	GISAID
G476S	hCoV-19/USA/WA-S28/2020	EPI_ISL_417081	GISAID
V483A	hCoV-19/USA/WA-S529/2020	EPI_ISL_434289	GISAID
Q414E	hCoV-19/USA/AZ-TGEN-TG268099/2020	EPI_ISL_426500	GISAID
G446V	hCoV-19/Australia/VIC329/2020	EPI_ISL_426639	GISAID
A475V	hCoV-19/USA/AZ-TGEN-TG268282/2020	EPI_ISL_426504	GISAID
A520S	hCoV-19/USA/WA_0432/2020	EPI_ISL_426441	GISAID

194

195 **Antibody discovery and expression.** mAbs were generated from SARS-CoV-2 RBD specific  
196 memory B cells using single B cell isolation and cloning strategy<sup>17</sup>. For preparation of MW05 and  
197 MW07 recombinant antibodies, heavy chain and light chain plasmids were transiently co-  
198 transfected into HEK293 cells or stably expressed in CHO cells followed by purification with  
199 Protein A resin. Antibodies MW05/LALA and MW07/LALA were generated by introducing the  
200 LALA mutation (L234A and L235A) in the Fc region of IgG1 to abolish binding with FcγRs and  
201 prepared using the same protocol used for generation of wild-type mAbs.

202

203 **ELISA.** To access the binding of mAbs to recombinant proteins (SARS-CoV-2 RBD, SARS-CoV-  
204 2 RBD mutants, SARS-CoV-2 S1, SARS-CoV S1 (Cat: 40150-V08B1, Sino Biological), MERS-  
205 CoV S1 (Cat: 40069-V08B1, Sino Biological)), the proteins were first coated on 96 well ELISA

206 plates at 1  $\mu$ g/ml in 100  $\mu$ L at 4°C overnight. After blocking with 5% BSA in PBS, serially diluted  
207 mAbs were added to the plates and incubated for 60 min at 37°C. Plates were washed and secondary  
208 Ab Goat Anti-Human IgG Fc-HRP (Cat: 109-035-098, Jackson ImmunoResearch) was added. TMB  
209 was used for color development and absorbance at 450 nm was measured using a microplate reader.  
210 For the RBD/ACE2-hFc blocking assay, ACE2-hFc recombinant protein was coated on a 96 well  
211 ELISA plate at 0.75  $\mu$ g/ml in 100  $\mu$ L at 4°C overnight. Equal volumes (100 $\mu$ L + 100 $\mu$ L) of pre-  
212 incubated RBD-mFc/mAb complex (RBD-mFc concentration: 100 ng/ml, mAb concentrations  
213 between 40 to 0.00023  $\mu$ g/ml) were added to the plates and incubated for 60 min at 37°C. Plates  
214 were washed and secondary Ab Goat Anti-Mouse IgG Fc-HRP (Cat:115-035-071, Jackson  
215 ImmunoResearch) was added. TMB was used for color development and absorbance at 450 nm was  
216 measured using a microplate reader.

217

218 **Flow cytometry assay.** The binding of MW05 and MW07 to S protein expression on cell surface  
219 was assessed by FACS. HEK293 cells were transiently transfected by SARS-CoV-2 Spike  
220 expression plasmid (Cat: VG40589-UT, Sino Biological) for 24 to 48 hours. Cells were then  
221 collected and blocked with 5% BSA for 30 min at RT. 3-fold serially diluted MW05, MW07, ACE2-  
222 hFc and isotype control antibody were added into cells ( $2 \times 10^5$  cells/sample in 100  $\mu$ L) and  
223 incubated for 60 min on ice. After washing twice with 1  $\times$  PBS, cells were stained with 1/200 diluted  
224 Goat Anti human IgG Fc-FITC antibody (Cat: F9512, Sigma) for 45 min and analyzed using flow  
225 cytometry (CytoFLEX, Beckman Coulter). The Fc $\gamma$ R expression profiles of Raji, THP-1 and K562  
226 were determined by FACS. Cells were collected and washed twice with 1 $\times$ PBS, then blocked with  
227 Fc receptor blocking solution buffer (Cat: MX1505, Maokang Biological) for 30 min at RT. Then

228 10  $\mu$ L anti-Fc $\gamma$ RI antibody-FITC (Cat: 10256-R401-F, Sino Biological), anti-Fc $\gamma$ RIIa antibody-  
229 FITC (Cat: 10374-MM02-F, Sino Biological), anti-Fc $\gamma$ RIIIa antibody-FITC (Cat: 10389-MM41-F,  
230 Sino Biological) and FITC-labeled anti-Fc $\gamma$ RIIb antibody (Cat: NBP2-14905, Biotechne; Cat:  
231 MX488AS100-1KT, Sigma-Aldrich) were added into cells (1 $\times$ 10<sup>6</sup> cells/sample in 100  $\mu$ L) and  
232 incubated for 60 min at 2-6°C and analyzed using flow cytometry (CytoFLEX, Beckman Coulter).

233

234 **Surface plasmon resonance (SPR).** SPR measurements were performed at room temperature using  
235 a BIAcore S200 system with CM4 biosensor chips (GE Healthcare). For all measurements, a buffer  
236 consisting of 150 mM NaCl, 10 mM HEPES, 3 mM EDTA, pH 7.4 and 0.005% (v/v) Tween-20 was  
237 used as running buffer. All proteins were exchanged into this buffer in advance. The blank channel  
238 of the chip served as the negative control. SARS-CoV-2 S1 recombinant protein was captured on  
239 the chip at 175 response units. Gradient concentrations of MW05 Fab or MW07 Fab (from 200 nM  
240 to 6.25 nM with 2-fold dilution) were then flowed over the chip surface. After each cycle, the sensor  
241 was regenerated with Gly-HCl (pH 1.5). The affinity was calculated using a 1:1 (R<sub>max</sub> Local fit)  
242 binding fit model with BIAevaluation software.

243

244 **Neutralization assay.** SARS-CoV-2 pseudovirus was prepared and provided by the Institute for  
245 Biological Product Control, National Institutes for Food and Drug Control (NIFDC)<sup>18</sup>. The TCID<sub>50</sub>  
246 was determined by the transduction of pseudovirus into Huh7 cells. For pseudovirus neutralization  
247 assay, 100  $\mu$ L of mAbs at different concentrations were mixed with 50  $\mu$ L supernatant containing  
248 500 TCID<sub>50</sub> pseudovirus. The mixture was incubated for 60 min at 37 °C, supplied with 5% CO<sub>2</sub>.  
249 All mAbs were tested in concentrations ranging from 0.55 ng/mL to 28  $\mu$ g/mL in the context of

250 Huh7 cells. 100  $\mu$ L of Huh7 cell suspension ( $2 \times 10^5$  cells/mL) was then added to the mixtures of  
251 pseudoviruses and mAbs for an additional 24 h incubation at 37 °C. Then, 150  $\mu$ L of supernatant  
252 was removed, and 100  $\mu$ L luciferase detecting regents (Promega) was added to each well. After 2  
253 mins incubation, each well was mixed 10 times by pipetting, and 150  $\mu$ L of the mixture was  
254 transferred to a new microplate. Luciferase activity was measured using a microplate luminometer  
255 (ThermoFisher). The 50% neutralization titer (NT<sub>50</sub>) was calculated using GraphPad Prism 7.0. For  
256 SARS-CoV-2 authentic virus neutralization assay, Vero E6 cells were diluted and seeded into a 96-  
257 well plate with  $1 \times 10^4$  cells/well in 100  $\mu$ L volume at 37 °C. 16 h later, cells were washed by 1 $\times$  PBS  
258 for 3 times and added diluted antibodies in equal volume with the concentration ranging from 0.1  
259  $\mu$ g/mL to 100  $\mu$ g/mL. 100 TCID<sub>50</sub> SARS-CoV-2 authentic virus was used for each well. Meanwhile,  
260 a control group without antibody was set up. A virus back-titration was performed to assess the  
261 correct virus titer used in each experiment. Cytopathic effect of each well was monitored every day  
262 and photographed at day 3 or day 4 after virus infection. All experiments were conducted following  
263 the standard operating procedures of the approved BSL-3 facility.

264

265 **Antibody-dependent enhancement (ADE) assay.** The ADE assays were performed using Raji,  
266 THP-1 and K562 cell lines. 25  $\mu$ L of 2-fold serially diluted mAbs were mixed with 25  $\mu$ L  
267 supernatant containing 250 TCID<sub>50</sub> pseudovirus. The mixture was incubated for 60 min at 37 °C,  
268 supplied with 5% CO<sub>2</sub>. All mAbs were tested in the concentrations ranging from 6000 to 23.4 ng/mL.  
269 100  $\mu$ L of THP-1, Raji and K562 cells at the density of  $2 \times 10^6$  cells/mL were added to the mixtures  
270 of pseudoviruses and mAbs for an additional 24 h incubation. Then, same volume of luciferase  
271 detecting regents (Promega) was added to each well. After 2 mins incubation, the luciferase activity

272 was measured using a microplate luminometer (Thermo Fisher).

273

274 **Animal experiments.** All animal experiments were performed according to the procedures

275 approved by the Chinese Academy of Sciences and complied with all relevant ethical regulations

276 regarding animal research. Nine 6 or 7 year-old rhesus monkeys (3 females and 6 males) were

277 divided into 3 groups: a control group (one female and two males), a pre-exposure group (one female

278 and two males) and a post-exposure group (one female and two males). Rhesus monkeys in the

279 control group were injected with 20 mg/kg negative control antibody. For the prophylactic study,

280 monkeys in the pre-exposure group were given a single dose of 20 mg/kg MW05/LALA antibody

281 intravenously one day before being challenged with  $1 \times 10^5$  TCID<sub>50</sub> SARS-CoV-2 via intratracheal

282 routes. For the therapeutic study, monkeys in the post-exposure group were administrated with a

283 single dose of 40 mg/kg MW05/LALA antibody intravenously one day after challenged with  $1 \times 10^5$

284 TCID<sub>50</sub> SARS-CoV-2 via intratracheal routes. Body weight and body temperature were monitored

285 every day. Oropharyngeal, nasal and rectal swabs were collected for 7 days. Blood samples were

286 collected. White blood cells (WBC), neutrophils (NEUT), lymphocytes (LYMPH) and monocytes

287 (MONO) were assessed for all monkeys. Swabs were placed into 1 mL of DMEM after collection.

288 Viral RNA was extracted by the QIAamp Viral RNA Mini Kit (Qiagen) according to the

289 manufacturer's instructions. RNA was eluted in 50  $\mu$ L of elution buffer and used as the template for

290 RT-PCR. The pairs of primers were used targeting S gene: RBD-qF1: 5'-

291 CAATGGTTAACAGGCACAGG-3'; RBD-qR1: 5'-CTCAAGTGTCTGTGGATCACG-3'. 2  $\mu$ L

292 of RNA were used to verify the RNA quantity by HiScript® II One Step qRT-PCR SYBR® Green

293 Kit (Vazyme Biotech Co., Ltd) according to the manufacturer's instructions. The amplification was

294 performed as follows: 50°C for 3 min, 95°C for 30 s followed by 40 cycles consisting of 95°C for  
295 10 s, 60°C for 30 s, and a default melting curve step in an ABI step-one machine (14).

296

297 **Histopathology and Immunohistochemistry.** Animal necropsies were performed according to a  
298 standard protocol. Samples for histological examination were stored in 10% neutral-buffered  
299 formalin for 7 days, embedded in paraffin, sectioned and stained with hematoxylin and eosin or  
300 Masson's trichrome prior to examination by light microscopy.

301

302 **Data availability.** Further information and requests for resources and reagents should be directed  
303 to and will be fulfilled by the corresponding author Xun Gui (xun.gui@mabwell.com).

304

305

306 **References**

- 307 1 Zhou, P. *et al.* A pneumonia outbreak associated with a new coronavirus of  
308 probable bat origin. *Nature* **579**, 270-273, doi:10.1038/s41586-020-2012-7  
309 (2020).
- 310 2 Wang, C., Horby, P. W., Hayden, F. G. & Gao, G. F. A novel coronavirus outbreak  
311 of global health concern. *Lancet* **395**, 470-473, doi:10.1016/S0140-  
312 6736(20)30185-9 (2020).
- 313 3 Galluccio, F. *et al.* Treatment algorithm for COVID-19: a multidisciplinary point of  
314 view. *Clin Rheumatol*, doi:10.1007/s10067-020-05179-0 (2020).
- 315 4 Chen, L., Xiong, J., Bao, L. & Shi, Y. J. T. L. I. D. Convalescent plasma as a potential  
316 therapy for COVID-19. **20**, 398-400 (2020).
- 317 5 Shen, C. *et al.* Treatment of 5 critically ill patients with COVID-19 with  
318 convalescent plasma. **323**, 1582-1589 (2020).
- 319 6 Sui, J. *et al.* Potent neutralization of severe acute respiratory syndrome (SARS)  
320 coronavirus by a human mAb to S1 protein that blocks receptor association. **101**,  
321 2536-2541 (2004).
- 322 7 ter Meulen, J. *et al.* Human monoclonal antibody as prophylaxis for SARS  
323 coronavirus infection in ferrets. **363**, 2139-2141 (2004).
- 324 8 Corti, D. *et al.* Protective monotherapy against lethal Ebola virus infection by a

325 potently neutralizing antibody. **351**, 1339-1342 (2016).  
326 9 Moekotte, A. *et al.* Monoclonal antibodies for the treatment of Ebola virus disease.  
327 **25**, 1325-1335 (2016).  
328 10 Saphire, E. O., Schendel, S. L., Gunn, B. M., Milligan, J. C. & Alter, G. J. N. i.  
329 Antibody-mediated protection against Ebola virus. **19**, 1169-1178 (2018).  
330 11 Li, Y. *et al.* A humanized neutralizing antibody against MERS-CoV targeting the  
331 receptor-binding domain of the spike protein. **25**, 1237-1249 (2015).  
332 12 Du, L. *et al.* The spike protein of SARS-CoV—a target for vaccine and therapeutic  
333 development. **7**, 226-236 (2009).  
334 13 Wang, Q., Wong, G., Lu, G., Yan, J. & Gao, G. F. J. A. r. MERS-CoV spike protein:  
335 Targets for vaccines and therapeutics. **133**, 165-177 (2016).  
336 14 Shi, R. *et al.* A human neutralizing antibody targets the receptor binding site of  
337 SARS-CoV-2. **1-8** (2020).  
338 15 Liu, L. *et al.* Anti-spike IgG causes severe acute lung injury by skewing  
339 macrophage responses during acute SARS-CoV infection. **4** (2019).  
340 16 Wan, Y. *et al.* Molecular mechanism for antibody-dependent enhancement of  
341 coronavirus entry. **94** (2020).  
342 17 Ju, B. *et al.* Human neutralizing antibodies elicited by SARS-CoV-2 infection. **1-8**  
343 (2020).  
344 18 Nie, J. *et al.* Establishment and validation of a pseudovirus neutralization assay for  
345 SARS-CoV-2. **9**, 680-686 (2020).  
346

347

348

349 **Acknowledgements:** We thank all colleagues from National Biosafety Laboratory (Wuhan), CAS  
350 for their support during the study. We thank Dr. Zhou Yi-Wu for his assistance in the  
351 histopathological analysis. We are grateful to Dr. Dayong Tian and Dr. Qi An from Shanghai King-  
352 cell Biotechnology Co. Ltd. for helping us performing the SARS-CoV-2 authentic virus neutralizing  
353 assays in the P3 laboratory. We thank Ms. Hongyuan Ren and Mr. Pan Gao for their helping in  
354 measuring the affinities in SPR assay. We thank Dr. Yu Mao and Ms. Wenlu Liang for the stimulating  
355 discussions.

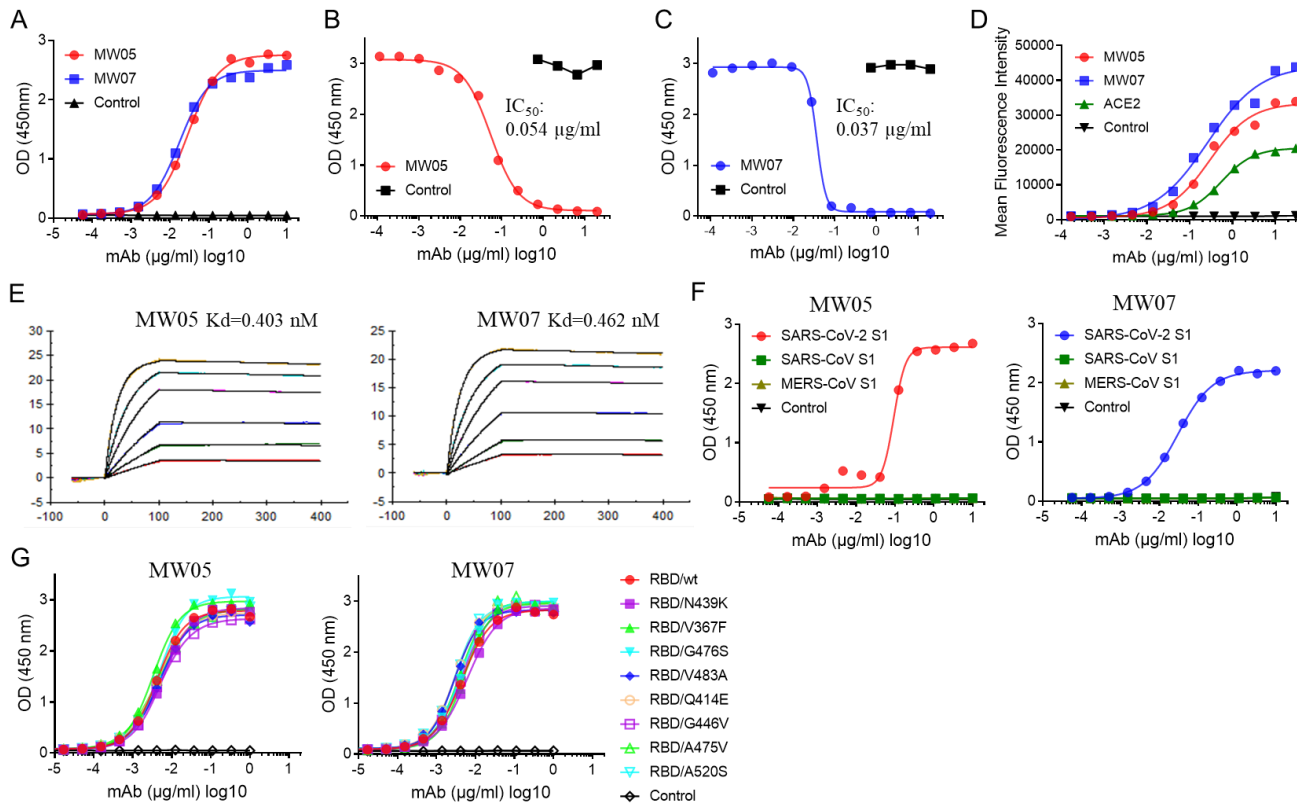
356 **Funding:** This work was supported by National Key R&D Program (2020YFC0848600).

357 **Author contributions:** D.L, J.Z, X.G. and S.W. initiated and coordinated the project. R.W. and S.J.

358 analyzed antigen sequences, expressed and purified recombinant proteins. Z.L., M.W., and P.T.  
359 expressed and purified antibodies. R.W. and S.J. performed the binding and blocking assays. B.C.  
360 and W.J. performed the pseudovirus neutralization assays. C.G. and W.J. checked the expression  
361 profile of Fc $\gamma$ Rs. W.H. and L.W. designed and supervised the SARS-CoV-2 pseudovirus tests. X.G.,  
362 B.C., W.J. and C.G. designed and performed the ADE experiments. G.L, A.W. and B.C supervised  
363 the protein quality control work. Z.Y., Y.P., C.S., X.H., Y.Y. carried out the monkey studies with the  
364 help from H.Z., Y.C. and G.G. J.M. and Y.C. performed histopathology and immunohistochemistry  
365 assays. S.C performed the Sars-CoV-2 mutants sequence data analysis and design work. X.G., S.W.,  
366 S.C. and J.Z. analyzed and prepared the manuscript with input from all authors.

367 **Competing interests:** X.G., S.W., R.W., S.J., W.J. and C.G. are listed as inventors on the licensed  
368 patents for MW05 and MW07. S.W., R.W., S.J., M.W., W.J., Z.L., C.G., B.C., P.T., J.Z., X.G. and  
369 D.L. are employees of Mabwell (Shanghai) Bioscience Co., Ltd. and may hold shares in Mabwell  
370 (Shanghai) Bioscience Co., Ltd. The other authors declare no competing interests.

**Figure 1**

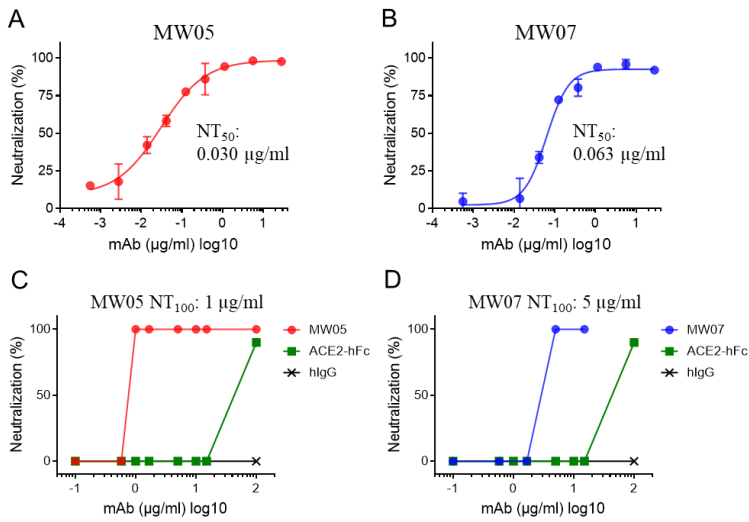


371 **Fig. 1. MW05 and MW07 disrupting the interaction of SARS-CoV-2 RBD with hACE2**

372 **receptor. (A)** The binding abilities of MW05 and MW07 to SARS-CoV-2 RBD recombinant  
373 protein were assessed by ELISA. **(B and C)** The ability of MW05 and MW07 to block SARS-  
374 CoV-2 RBD interaction with ACE2 was evaluated by competition ELISA. **(D)** The binding of  
375 MW05 and MW07 to SARS-CoV-2 S protein expressed on HEK293 cells was measured by  
376 FACS. **(E)** The dissociation constants ( $K_d$ ) of MW05 and MW07 to SARS-CoV-2 S1  
377 recombinant protein were measured using a BIACore S200 system. **(F)** The cross-reactivities  
378 of MW05 and MW07 to SARS-CoV-2, SARS-CoV and MERS-CoV recombinant S1  
379 subunit of spike proteins (S1) were tested by ELISA. **(G)** The binding of MW05 and MW07 to  
380 RBD recombinant proteins of SARS-CoV-2 mutated strains.

381

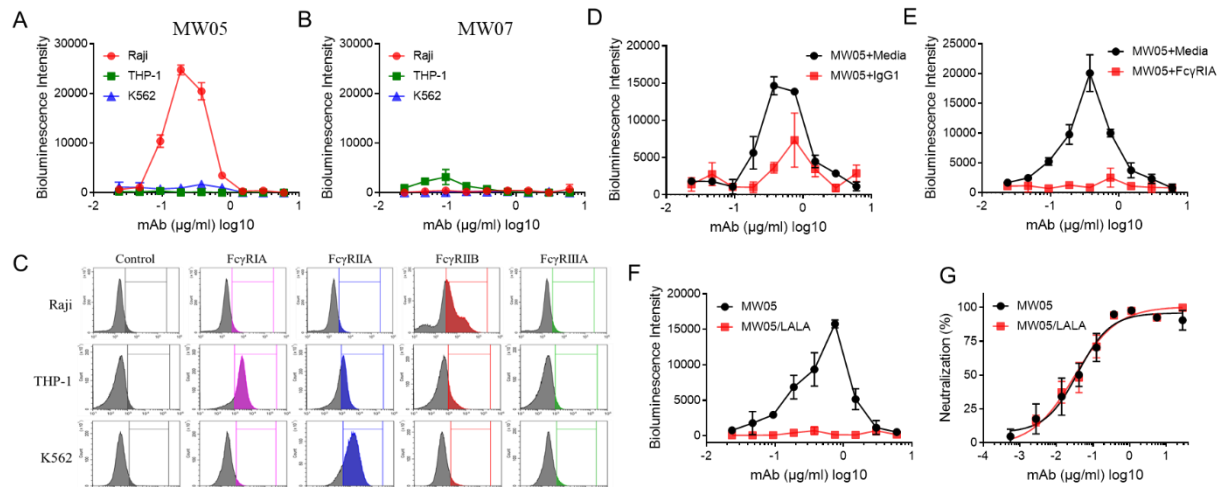
**Figure 2**



382 **Fig. 2. Neutralizing activities of MW05 and MW07. (A and B) SARS-CoV-2 pseudovirus**  
383 neutralizing activities of MW05 and MW07 were evaluated on Huh7 cells. 50% neutralization  
384 titer (NT<sub>50</sub>) was calculated by fitting the luciferase activities from serially diluted antibodies to  
385 a sigmoidal dose-response curve. (C and D) SARS-CoV-2 authentic virus neutralizing activities  
386 of MW05 and MW07 were evaluated using Vero E6 cells. 100% neutralization titer (NT<sub>100</sub>)  
387 was labeled accordingly.

388

**Figure 3**



389 **Fig. 3. Crosslinking of Fc and FcγR contributing to ADE activities of MW05. (A and B)**

390 ADE activities of MW05 and MW07 were assessed using SARS-CoV-2 pseudovirus.

391 Pseudoviruses pre-incubated with serially diluted mAb mixture were added to Raji, THP-1 and

392 K562 cells to evaluate their ability to enhance infection. RPMI 1640 media containing 10%

393 FBS was used as negative control. (C) ADE activities of MW05 on Raji cells pre-treated with

394 media or 400 μg/mL irrelevant hIgG1 were assessed using SARS-CoV-2 pseudovirus. (D) ADE

395 activities of MW05 pre-incubated with media or 80 μg/mL FcγRIA were assessed on Raji cells

396 using SARS-CoV-2 pseudovirus. (E) The ADE activities of MW05 and MW05/LALA on Raji

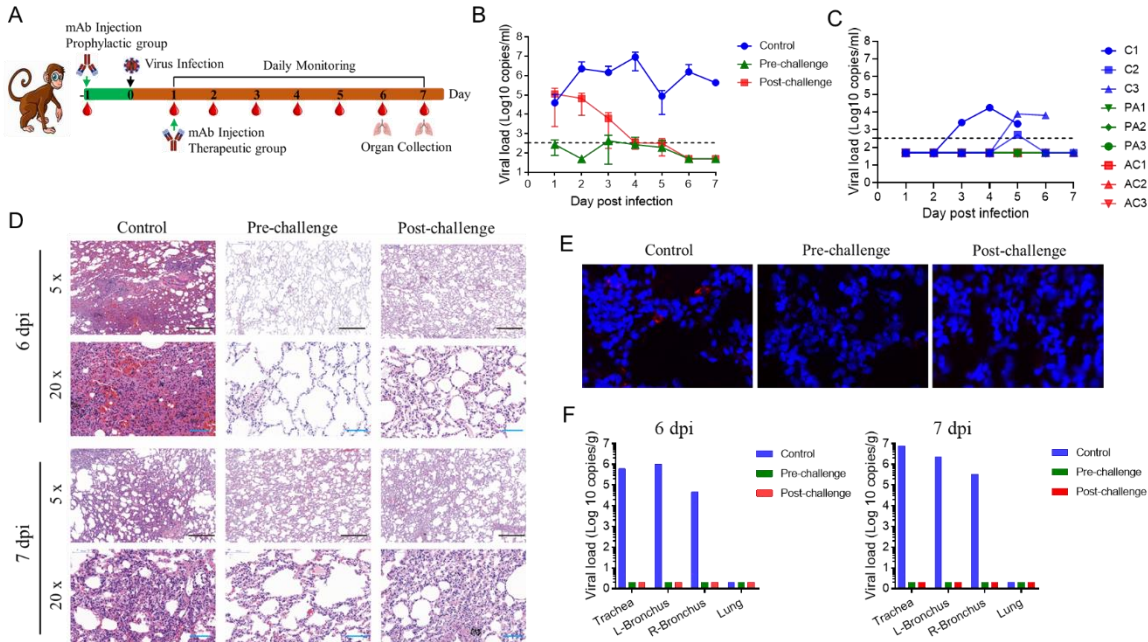
397 cells were compared using SARS-CoV-2 pseudovirus. (F) The pseudovirus neutralizing

398 activities of MW05 and MW05/LALA on Huh7 cells were measured.

399

400

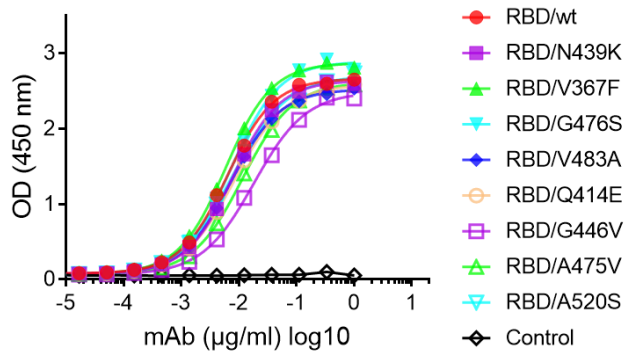
**Figure 4**



401 **Fig. 4. Prophylactic and therapeutic effects of MW05/LALA. (A)** A schematic of the  
402 experimental *in vivo* set up. Nine rhesus monkeys were divided into pre-challenge  
403 (prophylactic), post-challenge (therapeutic) and control groups with 3 animals in each group.  
404 Before virus challenge, the monkeys in the pre-challenge group were injected intravenously  
405 with a single dose of 20 mg/kg MW05/LALA . One day later, all monkeys were challenged  
406 with  $1 \times 10^5$  TCID<sub>50</sub> SARS-CoV-2 via intratracheal intubation. A single dose of 40 mg/kg  
407 MW05/LALA was administered to each animal in the post-challenge group on day 1 post  
408 challenge. Monkeys in the control group were given 20 mg/kg irrelevant hIgG1 one day before  
409 virus challenge. **(B)** Viral titer of oropharyngeal swabs at the indicated time points were  
410 evaluated using qRT-PCR. Data are average values from three monkeys (n=3) for the first 5  
411 days, from two monkeys (n=2) for 6 dpi, and from one monkey (n=1) for 7 dpi. The line for  
412 limit of detection is labeled. **(C)** Viral titer of rectal swabs at the indicated time point were  
413 evaluated by qRT-PCR. “C” indicates the control group, “PA” indicates the pre-challenge

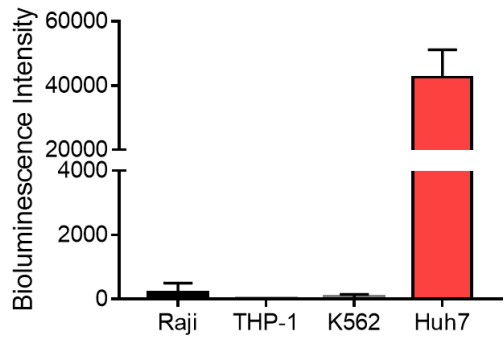
414 group and “AC” indicates the post-challenge group. **(D)** Histopathology and  
415 immunohistochemical examination of lung tissues from pre-challenge, post-challenge and  
416 control monkeys. **(E)** Immunohistochemical analysis of SARS-CoV-2 protein expression in  
417 lung tissues from pre-challenge, post-challenge and control monkeys. **(F)** Viral load analysis  
418 of trachea, bronchus and lung tissues of experimental animals. L-Bronchus means left bronchus;  
419 R-Bronchus means right bronchus.

420



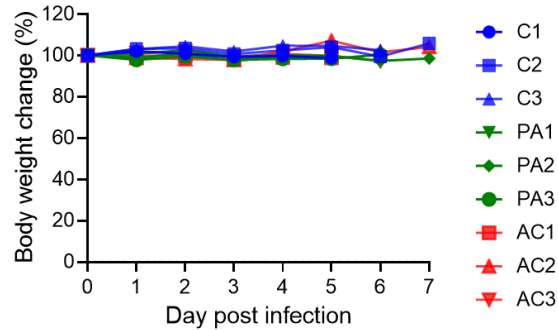
421 **Extended Data Fig. 1 Binding of ACE2 to different SARS-CoV-2 RBD mutants by**  
422 **ELISA.** RBD recombinant proteins were coated on 96-well plates. Human ACE2-mFc was  
423 then added into plates to check the binding.

424



425 **Extended Data Fig. 2 The infection of SARS-CoV-2 pseudovirus in Raji, THP-1, K562 and**

426 **Huh7 cells.**

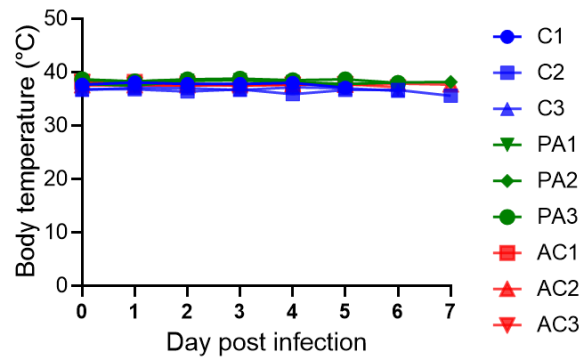


427 **Extended Data Fig. 3 The body weight of each monkey was checked every day. “C”**

428 indicates the control group, “PA” indicates the pre-challenge group and “AC” indicates the

429 post-challenge group.

430

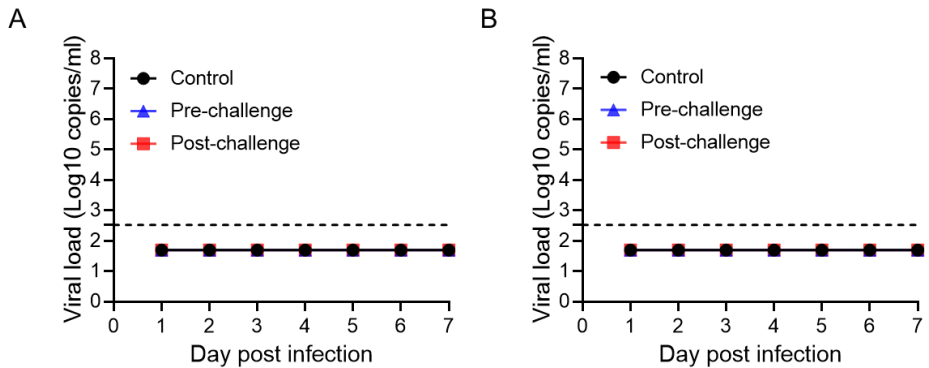


431 **Extended Data Fig. 4 The body temperature of each monkey was checked every day. “C”**

432 indicates the control group, “PA” indicates the pre-challenge group and “AC” indicates the

433 post-challenge group.

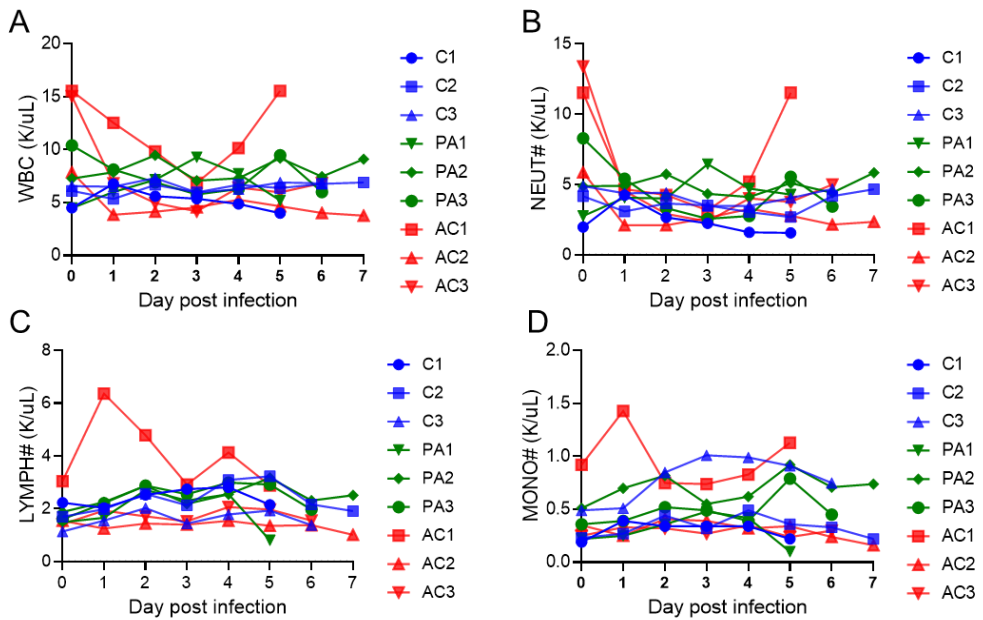
434



435 **Extended Data Fig. 5 Viral titer of nasal swabs (A) or blood samples (B) of all monkeys**

436 **were evaluated by qRT-PCR.**

437



438 **Extended Data Fig. 6 White blood cells (A), neutrophils (B), lymphocytes (C) and**  
439 **monocytes (D) in each monkey were monitored every day. "C" indicates the control group,**  
440 **"PA" indicates the pre-challenge group and "AC" indicates the post-challenge group.**

441